Korean Chem. Eng. Res., 64(1), 105150 (2026)
https://doi.org/10.9713/kcer.2026.64.1.105150
PISSN 0304-128X, EISSN 2233-9558

Evaluation of Physicochemical Parameters in Methylene Blue Adsorption on to Activated Biochar (ABC)

Chebbi Rachid*, Fadel Ammar*, Souifi Imane*, Salma Samidin and Wan Nor Roslam Wan Isahak****

**Chemical and Environmental Process Engineering Laboratory, University of Biskra, PO Box 145, Biskra, 07000, Algeria*
***Department of Chemical and Process Engineering, Faculty of Engineering and Built Environment,*
Universiti Kebangsaan Malaysia, 43600 UKM Bangi, Selangor, Malaysia

(Received 2 May 2025; Received in revised from 28 August 2025; Accepted 4 December 2025)

Abstract – The increasing focus on environmental preservation and protection necessitates innovative methods and technologies to address various forms of waste. Adsorption using activated carbon is a well-established and promising approach for removing pollutants, particularly methylene blue, from wastewater. This study aims to develop a carbon-rich adsorbent derived from biomass-based date seeds and transform it into activated biochar (ABC). Important physicochemical parameters, including activation temperature, mass loss during activation, biochar particle sizes, initial methylene blue concentration, adsorption time, and adsorbent mass were examined in detail to determine their effects on adsorption capacity. The activated biochar's morphological structure and functional groups were characterized using SEM, XRD, and FTIR techniques. The results revealed that the optimal activation temperature for producing ABC was 1000 °C, yielding 99.15% efficiency and an adsorption capacity (qe) of 19.83 mg/g. The effective adsorption time was determined to be 60 minutes, achieving an adsorption efficiency of 96.16% and a q_e value of 9.61 mg/g.

Key words: Date seeds, Activation temperature, Activated biochar, Adsorption, Methylene blue

1. Introduction

Despite in trace amount or dissolved in water, the dyes released by factories and industries can interact with daily human activities, posing serious health risks such as childhood hyperactivity, eczema, asthma, attention deficit disorder, and potentially cancer [1-3]. This growing warning signals the need for global environmental protection and pollution mitigation efforts. In order to reduce the toxicity and related health concerns of pollutants like pesticides, volatile organic compounds (VOCs), and dyes, innovative, efficient, and sustainable treatment technologies must be urgently developed. These initiatives align with Sustainable Development Goal 6, emphasizing the protection of freshwater resources and the advancement of universal access to sustainable water management systems.

Methylene blue (MB) is widely utilized chemical across the industries such as textiles, food production, and pharmaceuticals. However, the release and dissolution of methylene blue at elevated concentrations into terrestrial water and atmosphere, significantly increases its environmental toxicity. It should be noted that the persistent and long-term presence of methylene blue in aquatic systems cause devastating damage to the ecosystems. This pressing issue necessitates for immediate development of transformative and sustainable remediation solutions to mitigate its alarming impacts. Many technologies have been developed for dye removal, including coagulation [4], oxidation [5], ultra-filtration, electrochemical processes, and photocatalysis [6-10]. Among these, adsorption has emerged as the most effective technique for removing dyes, because of the simplicity in design and operation, cost-effectiveness, versatility, and enabling the removal of pollutants in solid, liquid, and gaseous forms [11,12]. The efficiency of adsorption technique depends on critical factors such as the choice of adsorbent and adsorbate, as well as the physicochemical properties of the materials involved.

Notedly, activated carbon and biochar are most widely explored adsorbents currently due to their high pollutant removal rates, extensive pore structure, great surface area, and tunable functional groups [13-15]. Despite its effectiveness, the production of conventional activated carbon is energy-intensive and environmentally taxing, leading to the interest in sustainable alternatives derived from biomass. Green adsorbents derived from biomass and agricultural wastes offer a promising alternative, aligning with circular economy principles and reducing environmental impact. Biochar, a carbon-rich material produced through pyrolysis, considered as a sustainable raw material for bio adsorbent. Its low cost, and potential for chemical activation to enhance adsorption capabilities make it a compelling candidate for wastewater treatment. However, the optimization of biochar properties and the systematic evaluation of physicochemical parameters, such as the nature of activators, activation temperature, and adsorbent size, remain underexplored, creating a critical gap in the current research landscape [16,17].

The main objective of this work was to valorize the date seeds, a local material with no current economic value, by transforming them

---

[†] To whom correspondence should be addressed.
E-mail: am.fadel@univ-biskra.dz

into activated biochar (ABC), with economically valuable adsorbent. In this transformation chemical activators with zinc chloride ($ZnCl_2$) and sodium chloride (NaCl) were used at differences temperatures from 400°C to 1000°C, and physicochemical factors, including activation temperature, mass loss during activation, activator type, adsorbent size (1 mm and 250 μm), dye concentration, stirring time, and adsorption temperature were evaluated. Furthermore, the activated biochar (ABC) was characterized using advanced techniques such as Fourier-transform infrared spectroscopy (FTIR), X-ray diffraction (XRD), and Scanning electron microscopy (SEM).

2. Materials and Methods

2-1. Activated Biochar (ABC) Source

Date seeds were sourced from Deglet Baydha dates, harvested in the Sidi Khaled region of Biskra State, southern Algeria, North Africa (Fig. 1). The process of transforming these seeds into activated biochar (ABC) involved two main stages: pre-carbonization and carbonization with chemical activation, as described in Sections 2.1.1 and 2.1.2.

2-1-1. Pre-carbonization

The date seeds were initially dried at a room temperature *i.e.,* 30 °C for 8 hours. Subsequently, they were dried in the oven at 100 °C for 24 hours to ensure the complete removal of residual moisture.

2-1-2. Carbonization and Activation ($ZnCl_2$ and NaCl)

Dried date seeds were carburized at 200 °C for 2 hours. The synthesized biochar was ground and sieved to obtain particles of two sizes: 1 mm and 250 μm. Chemical activation was conducted using zinc chloride ($ZnCl_2$) and sodium chloride (NaCl) as activators. For $ZnCl_2$ activation, 10 g of biochar (BC) was impregnated in 15 mL of 0.1 N $ZnCl_2$ solution, followed by stirring for 15 min to ensure uniform distribution of the activating agent. The impregnated biochar was placed in a muffle furnace at 200 °C for 30 minutes under limited oxygen conditions. The material was subsequently calcined at different temperatures: 400 °C, 600 °C, 800 °C, and 1000 °C for 4 hours. After activation, the biochar obtained was washed many times with distilled water until a neutral pH (pH ≈ 7). Finally, the washed biochar was dried in the oven at 100 °C for 24 hours.

Fig. 1. Date seeds image extracted from Dagla Baydha.

For NaCl activation, the procedure was repeated using 7.5 mL of NaCl solution instead of $ZnCl_2$. The process was performed separately for the two biochar particle sizes (1 mm and 250 μm). The activated biochar (ABC) samples produced under these conditions were stored in containers for subsequent characterization and analysis.

Figure 2 illustrates the preparation steps involved in the production of activated biochar (ABC), describing the calcination process at different temperatures *i.e*., the stages from biochar (BC) to the final activated biochar (ABC).

2-2. Parametric Studies

The prepared activated biochar (ABC) was employed to remove methylene blue (MB) molecules from wastewater through adsorption. A stock solution of MB with a 10 mg/L initial concentration was prepared. About five (05) different concentrations were subsequently prepared for calibration to determine the absorbance peak wavelength (λ_{max}) of methylene blue using UV spectroscopy. The absorbance spectrum confirmed the maximum wavelength for methylene blue as λ_{max} = 663 nm (Fig. 3). ABC, derived from date seeds, was selected for adsorption and parameter studies.

2-2-1. Temperature effect on mass loss of activated biochar

10 g of biochar, in particle sizes of 250 μm and 1 mm, was prepared using $ZnCl_2$, NaCl as activators, and a control sample without an activator. The samples were subjected to calcination at temperatures

Fig. 2. Calcination process for activated biochar (ABC) at different temperatures: (a) Biochar (BC), (b) BC with activators at various temperatures, and (d) final activated biochar (ABC).

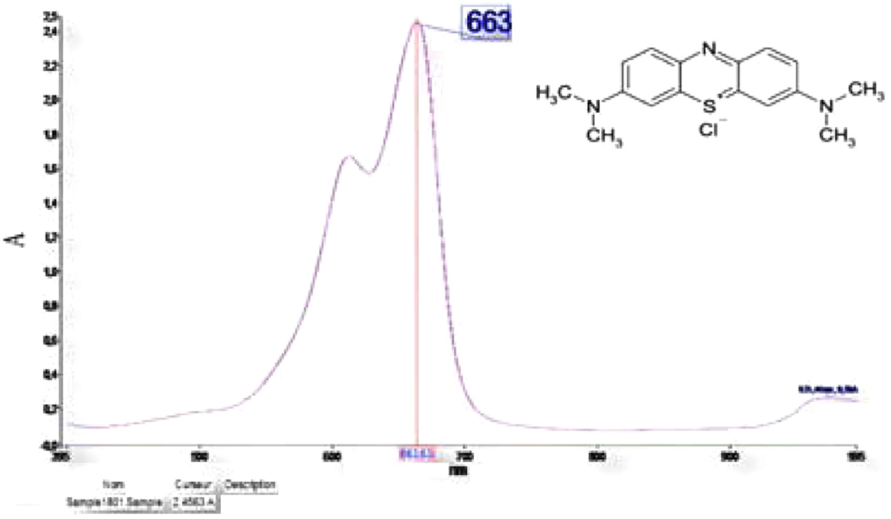

Fig. 3. Absorption spectrum of methylene blue measured by UV spectroscopy.

of 400 °C, 600 °C, 800 °C, and 1000 °C in a muffle oven under limited oxygen conditions to investigate the effect of temperature on mass loss. After each thermal treatment, the mass loss was recorded, and the results were used to analyze the influence of activation temperature and particle size on biochar decomposition.

2-2-2. Temperature effect on the adsorption phenomena

The adsorption capacity of methylene blue on activated biochar was evaluated at four calcination temperatures: 400 °C, 600 °C, 800 °C, and 1000 °C with $ZnCl_2$ and NaCl activators, as well as non-activated (natural) biochar for comparison. Two particle sizes (1 mm and 250 μm) were used for all activation conditions. For each experiment, 0.05 g of activated biochar was mixed with 250 mL of methylene blue solution at a 4.0 mg/L an initial concentration. The mixture was placed in a stirring apparatus and agitated with a speed of 200 rpm for 50 minutes at a controlled temperature of 27 °C to ensure proper mixing and interaction between the adsorbent and the adsorbate. Following the stirring phase, the solution was left to settle for 30 minutes to allow decantation. The equilibrium concentration (C_e) of MB in the filtrate was measured using UV spectroscopy. The adsorption yield (%) and adsorption capacity (q_e) of ABC were then calculated using the following equations [18]:

$$q_e = (C_0 - C_e) * V / m$$

$$\mathrm{Re}\,moval(\%) = \left[(C_0 - C_e) / C_0\right] \times 100$$

Where:

C_0: initial concentration (mg/L)
C_e: equilibrium concentration (mg/L)
V: volume of solution (L)
m: mass of adsorbent (g)

2-2-3. Concentration effect on the adsorption efficiency

To examine the effect of concentration, three methylene blue solutions (3, 7, and 9 mg/L) were prepared, each with a volume of 250 mL. For all the tests, 0.5 g of activated biochar prepared at 1000 °C was used as the adsorbent. The solutions were stirred at 200 rpm for 50 minutes at room temperature. After decantation for 30 minutes, the equilibrium concentration was determined using UV spectroscopy. The removal efficiency (%) and adsorption capacity were also calculated.

2-2-4. Contact time effect on adsorption

The effect of contact time on adsorption efficiency was evaluated by mixing 250 mL of 3 mg/L methylene blue solution with 0.075 g of activated biochar prepared at 1000 °C. The experiment was conducted using a "JAR TESTED" stirring apparatus at 200 rpm. The stirring times were set to 10, 30, 40, and 60 minutes. Following each time interval, the samples were decanted for 30 minutes, and the equilibrium concentration was measured. The removal yield and adsorption capacity were calculated for each stirring time.

2-2-5. Adsorption temperature effect

The influence of adsorption temperature on methylene blue removal was studied using three temperatures: 10 °C, 20 °C, and 40 °C. Three beakers, each containing 250 mL of a 3.0 mg/L methylene blue solution and 0.05 g of activated biochar, were stirred at 200 rpm for 50 minutes. Post-stirring, the solutions were allowed to settle for 30 minutes. Filtration was performed using a 0.45 μm filter paper for selected samples to recover the biochar. The equilibrium concentration and the adsorption capacity (q_e) were determined.

3. Results and Discussion

3-1. Characterization of Biochar and Activated Biochar

Activated biochar (ABC) and Biochar (BC) were characterized to evaluate their composition, morphology, and functional groups using Scanning electron microscopy (SEM), Energy-dispersive X-ray spectroscopy (EDX), X-ray diffraction (XRD), and Fourier-transform

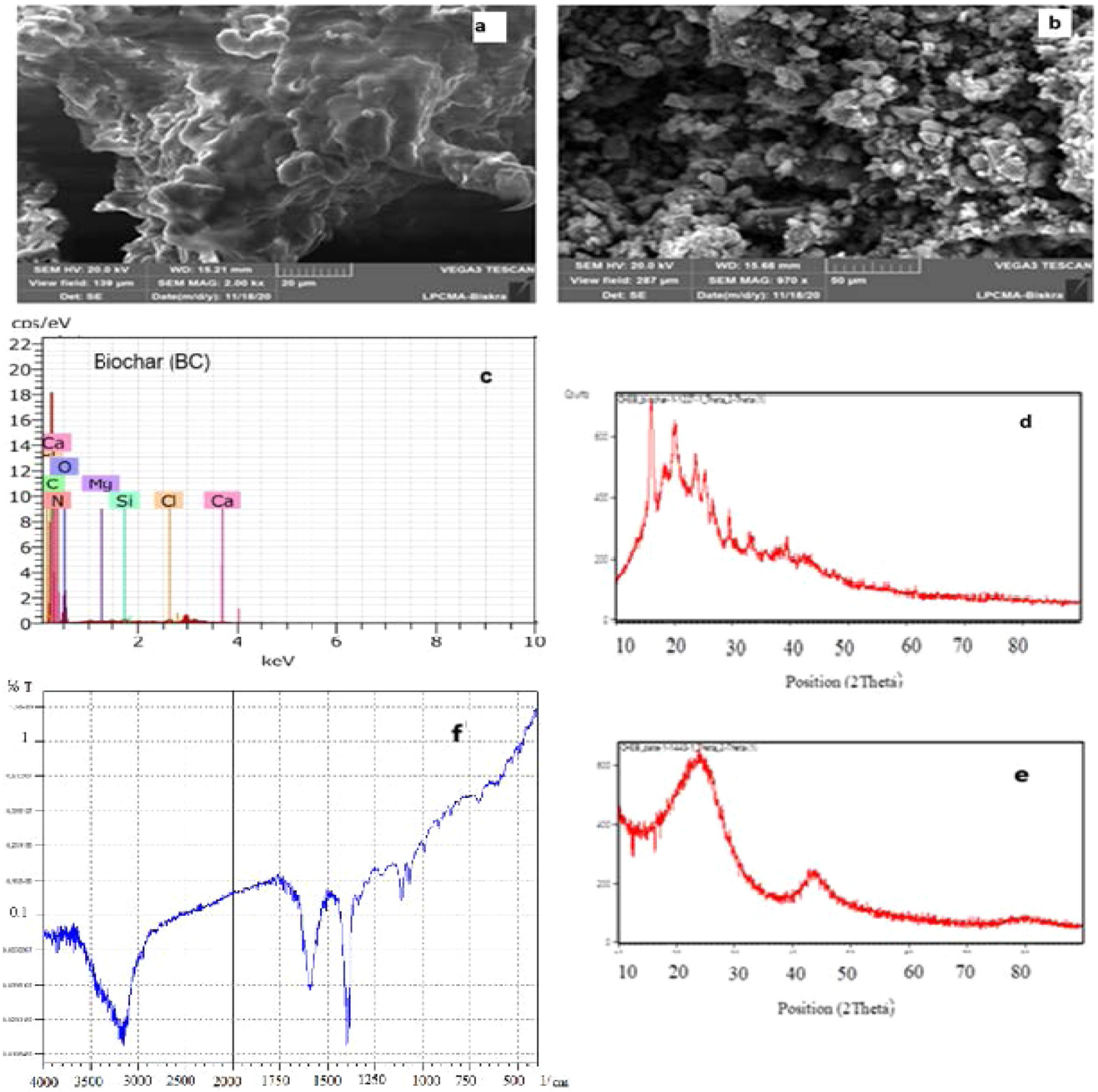

Fig. 4. Characterization of activated biochars: (a) SEM of BC without chemicals activation at 200 °C and (b) ABC at 1000 °C using $ZnCl_2$, (c) EDX of BC (d) XRD of BC without chemicals activated at 200 °C and (e) ABC at 1000 °C, (f) FTIR ofABC at 1000 °C using $ZnCl_2$.

infrared spectroscopy (FTIR) techniques.

The scanning electron microscopy (SEM) of biochar without chemical activation at 200 °C is depicted in Fig. 4a, which is comparatively homogenous and smooth with no discernible porosity. On the other hand, the surface morphology of activated biochar made with $ZnCl_2$ as the activator and heated to 1000 °C is shown in Fig. 4b. It was observed that upon activation by $ZnCl_2$, a highly porous structure with numerous cavities and interconnected voids was formed. These structural changes were attributed to the volatilization and removal of mineral components such as silicon (Si), nitrogen (N), and chlorine

Table 1. EDX analysis of biochar and activated biochar elements

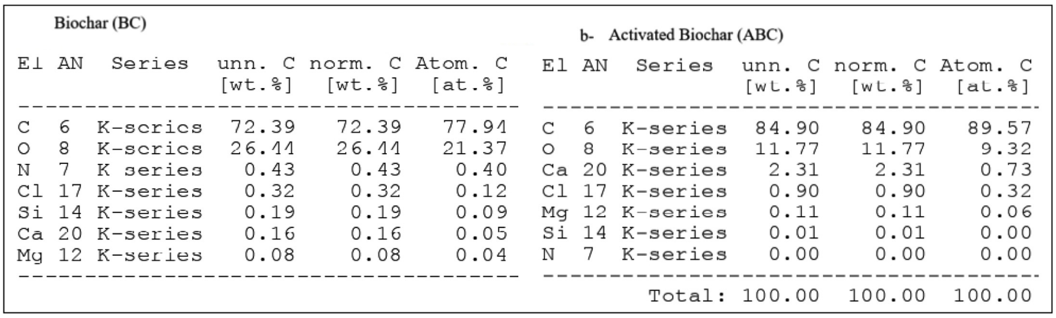

Biochar (BC)

b- Activated Biochar (ABC)

```
El AN  Series   unn. C norm. C Atom. C    El AN  Series   unn. C norm. C Atom. C
                [wt.%]  [wt.%]  [at.%]                    [wt.%]  [wt.%]  [at.%]
---------------------------------------   ---------------------------------------
C   6  K-scrics  72.39   72.39   77.94    C   6  K-series  84.90   84.90   89.57
O   8  K-scrics  26.44   26.44   21.37    O   8  K-series  11.77   11.77    9.32
N   7  K series   0.43    0.43    0.40    Ca 20  K-series   2.31    2.31    0.73
Cl 17  K-series   0.32    0.32    0.12    Cl 17  K-series   0.90    0.90    0.32
Si 14  K-series   0.19    0.19    0.09    Mg 12  K-series   0.11    0.11    0.06
Ca 20  K-series   0.16    0.16    0.05    Si 14  K-series   0.01    0.01    0.00
Mg 12  K-series   0.08    0.08    0.04    N   7  K-series   0.00    0.00    0.00
---------------------------------------   ---------------------------------------
                                                   Total: 100.00  100.00  100.00
```

(Cl) during chemical activation and calcination, which can be identified as the elements C, O, Ca, Cl, Mg, Si, and N by EDX analysis from biochar (Fig. 4c), whereas after biochar activation some elements have gone as Si, Mg as shown in Table 1. This enhanced porosity was critical for improving the adsorption performance of activated biochar, as it increased the surface area available for interaction with adsorbates. The variations in BC and ABC's surface morphology demonstrated how chemical activation and high-temperature treatment created a porous structure appropriate for adsorption applications.

Activating with $ZnCl_2$ increased the surface specific area of biochar by supporting the formation of porous structure due to the breakdown of its molecular structure. Thus led to the formation of higher quantity of micropores and enhanced adsorption capacity. $ZnCl_2$ caused a swelling and broke down the original molecules within the biochar which created a more open, porous structure with significantly increased number of micropores and a higher pore volume.

$ZnCl_2$ acted as a Lewis acid, facilitating the disintegration of carbon chains and the formation of numerous pores of various sizes.

The remarkable ability of $ZnCl_2$ to improve structural properties was demonstrated by the increased porosity seen in activated biochar (ABC), which was consistent with findings from previous studies (MacHado et al. 2020). Machado et al reported that $ZnCl_2$ activation significantly improved pore development in biochars, increasing the surface area from 6.5 m^2/g in non-activated biochar to 545 m^2/g in $ZnCl_2$-activated biochar, thereby demonstrating the remarkable capacity of $ZnCl_2$ to enhance structural properties. Similar to this, $ZnCl_2$ activation, broke down the cellulose molecular bonds, encouraging the creation of mesopores while preserving structural stability—a characteristic that was visible in the porous network of ABC [19]. Therefore, this finding proved that chemical activation and heat treatment were crucial for increasing adsorption potential and was further demonstrated by the transformation from a thick, smooth charcoal surface to a highly porous, adsorbent-ready surface. Notably, larger adsorbate molecules were transported through the mesopores in ABC, while the macropores functioned as reservoirs, reducing mass transfer restrictions and enhancing overall effectiveness. These characteristics were particularly beneficial for applications such as methylene blue adsorption. The XRD pattern for biochar without chemical activation at 200 °C (Fig. 4d) revealed distinct diffraction peaks, indicating the presence of mineral impurities, such as calcium and phosphorus compounds, that persisted after carbonization. These crystalline characteristics demonstrated the restricted structural alterations brought by low-temperature pyrolysis in the absence of chemical activation. In contrast, the XRD pattern for activated biochar (Fig. 4e) showed broad diffraction peaks around $2\theta=24°$ and $44°$, corresponding to the (002) and (100) planes of amorphous carbon materials, respectively. The transition from sharp diffraction peaks in BC to broad peaks in ABC indicated the successful transformation into an amorphous structure, which was the characteristic of thermally and chemically activated carbon materials. Amorphous carbon was particularly advantageous for adsorption applications due to its increased surface irregularity and available spaces for adsorbate molecules. Furthermore, amorphous materials have more voids that can accommodate the molecules of the adsorbate, hence they were generally more suited for adsorption [20]. These findings aligned with previous studies [17,21], which emphasized the role of chemical activation and high-temperature treatment in enhancing structural properties.

The functional groups in ABC were identified using Fourier-transform infrared (FTIR) spectroscopy spanning the 400–4000 cm^{-1} range (Fig. 4f). Significant transmittance bands in the FTIR spectrum demonstrated the chemical functionalities brought by activation. The stretching vibrations of O-H bonds in hydroxyl groups, a crucial component influencing ABC's hydrophilic characteristic, were represented by the broad band seen at 3180 cm^{-1}. C=O stretching vibration in carboxylic acid groups was identified as the source of a clear peak located between 1600 and 1590 cm^{-1} [22-24]. The presence of oxygen-containing functional groups was further confirmed by other peaks at 1400 cm^{-1}, 1110 cm^{-1}, and 1070 cm^{-1} that correspond to C–O stretching vibrations [25-27]. According to Towfik, A. Saleh. (2018) [28], the presence of O–H and C–O functional groups improved ABC's adsorption capacity by offering active sites for interactions with adsorbates like methylene blue.

3-2. Effect of physicochemical parameters

3-2-1. Temperature effect on mass loss of activated biochar

Temperature effect on the mass loss of biochar (BC) during activation was evaluated for samples with different particle sizes (250 μm and 1 mm) and activation conditions ($ZnCl_2$, NaCl, and no activator). Each 10 g biochar sample was subjected to thermal treatment at 400 °C, 600 °C, 800 °C, and 1000 °C in an oven under limited oxygen conditions. The resulting mass losses are presented in Table 2, and the corresponding trends are illustrated in Fig. 5a (powdered BC, 250 μm) and Fig. 5b (granular BC, 1 mm). The results indicated that mass loss decreased as the activation temperature increased, regardless of the particle size or type of activator used. The variation in mass was strongly influenced by the temperature and the biochar particle size, with granular biochar (1 mm) showing higher mass loss compared to powdered biochar (250 μm). This trend suggested that larger particles experienced more

Table 2. Biochar mass loss at different temperatures and particle sizes for various activators

T (°C)	No Activator	$ZnCl_2$	NaCl	$ZnCl_2$	NaCl
	1 mm	1 mm	1 mm	250 μm	250 μm
400	1.77 g	3.3 g	1.85 g	2.25 g	1.95 g
600	1.56 g	2.55 g	1.75 g	1.94 g	1.79 g
800	1.30 g	1.34 g	1.45 g	0.88 g	0.98 g
1000	0.00 g	0.08 g	1.14 g	0.27 g	0.10 g

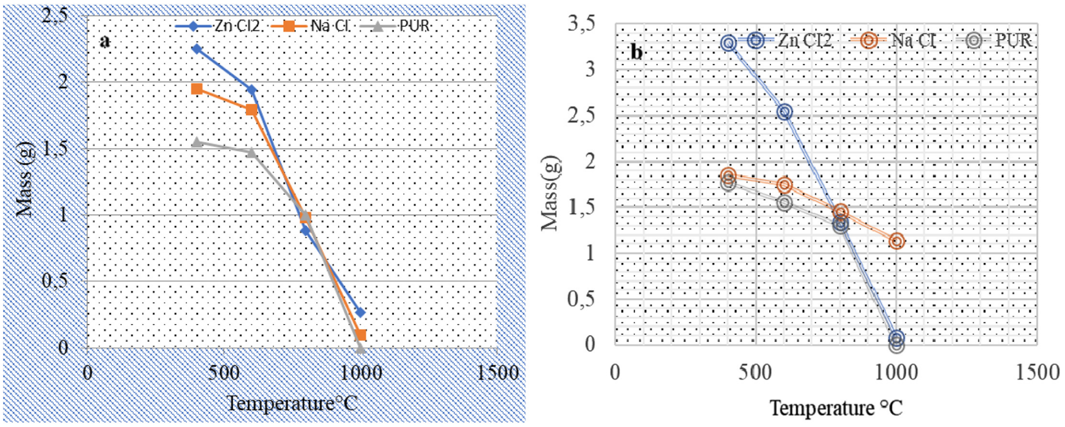

Fig. 5. Temperature effect on the mass loss of activated biochar (ABC) (a) powder (250 µm), and (b) granular (1 mm).

significant volatilization and decomposition at higher temperatures due to slower heat diffusion and the retention of volatiles within the particle core [28].

The pyrolysis temperature played a critical role in the release of volatile compounds, with higher temperatures resulting in greater mass loss. For instance, at 400 °C, the biochar mass decreased from 10 g to 3.3 g for granular biochar (1 mm) activated with $ZnCl_2$, while powdered biochar exhibited a reduction to 2.25 g. At 1000 °C, biochar activated with $ZnCl_2$ showed almost complete decomposition (0.08 g for 1 mm and 0.27 g for 250 µm), emphasizing the catalytic role of $ZnCl_2$ in enhancing thermal degradation and facilitating formation of porous formation [29]. Meanwhile, higher temperatures promoted more mass loss and more stable chemical formed, increasing the utility of biochar for a variety of uses [29,30].

Samples activated with NaCl or without activators demonstrated comparatively lower mass loss due to their weaker catalytic effects. The mass loss trends observed can be attributed to the volatilization of organic and inorganic components in the biochar during high-temperature activation. This finding proved that $ZnCl_2$ was more effective than NaCl as a chemical activator due to its strong catalytic properties and ability to enhance pore development during biochar activation. $ZnCl_2$ acted as a dehydrating agent, efficiently breaking down lignocellulosic structures and facilitating the release of volatiles, leading to higher mass loss and improved porosity. It promoted the formation of micropores and mesopores by aiding thermal decomposition and enhancing aromatic condensation, resulting in a stable, porous carbon structure ideal for adsorption applications. In contrast, NaCl exhibited weaker catalytic effects, creating less porosity and achieving lower mass loss, making it less effective for biochar activation, which was in agreement with Dehkhoda, et al. (2016) [33].

3-2-2. Temperature effect on adsorption phenomena

Figure 6 illustrates the variation in yield (R) and adsorption capacity (q_e) as a function of activation temperature. The results showed that q_e increased with rising activation temperature, reaching a maximum at 1000 °C with R=99.15% and q_e=19.83 mg/g, respectively. Meanwhile, the minimum values were observed at 400 °C, where R=86.4% and q_e=17.28 mg/g and q_e=17.28 mg/g. This increase in adsorption efficiency with temperature can be attributed to the enhanced effect of temperature on pore formation and structural modification of the biochar in the presence of chemical activators. Elevated temperatures promoted the development of micropores and mesopores, facilitating more effective adsorption [32-34].

Furthermore, the thermal degradation of biomass components, particularly cellulose and lignin, contributed significantly to the mass reduction and pore creation. The thermal decomposition of cellulose

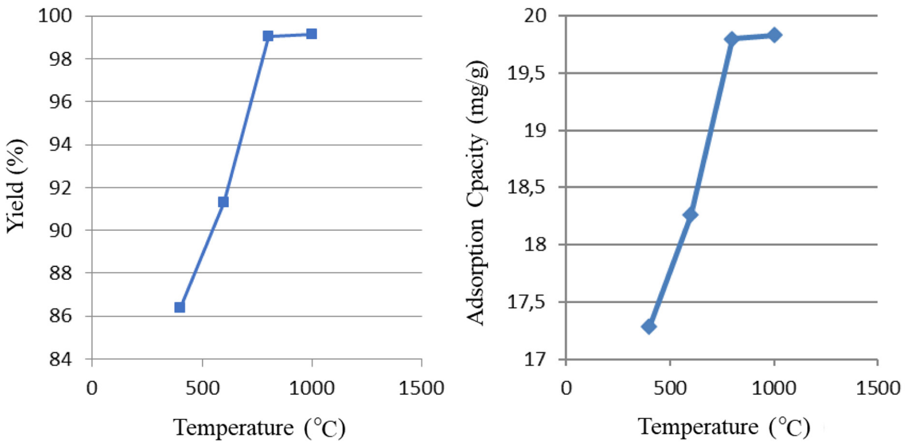

Fig. 6. Yield and adsorption capacity of methylene blue on activated biochar (ABC) at different temperatures.

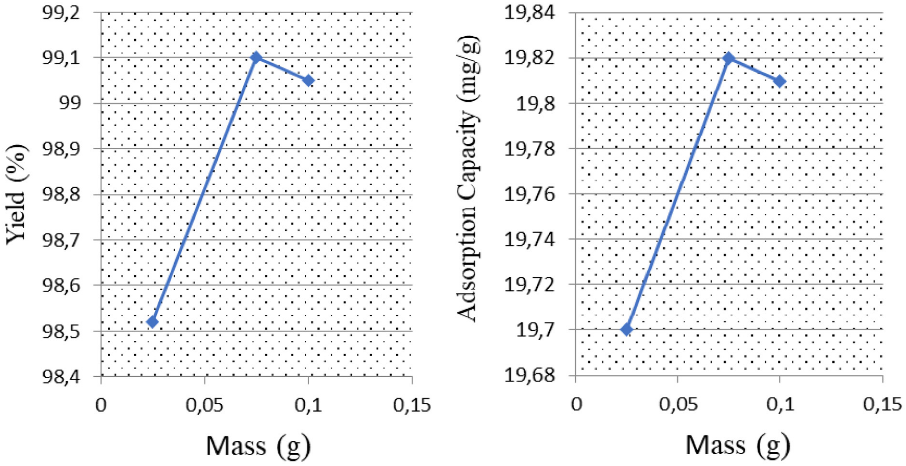

Fig. 7. Yield and adsorption capacity of methylene blue on activated biochar (ABC) at varying adsorbent masses.

occurred above 613 K, while lignin degradation primarily took place between 633 K and 1000 K [35]. These processes played a crucial role in increasing the surface area and adsorption capacity of activated biochar. Figure 7 depicts the relationship between ABC mass and the adsorption performance. The results showed that the removal efficiency (Y) reached 99.1%, with a slight variation in q_e values. The maximum capacity of 19.82 mg/g was observed at an adsorbent mass of 0.075 g, while at 0.025 g, q_e decreased slightly to 19.7 mg/g. This trend suggested that the optimal adsorbent mass ensured sufficient surface area for adsorption while avoiding oversaturation, which could lower adsorption efficiency due to limited available active sites.

3-2-3. Concentration effect on the adsorption efficiency

The results indicated that activated biochar adsorbed a significant quantity of methylene blue, with the clearest solution observed for the sample with an initial concentration of 3 mg/L. As shown in Fig. 8, the adsorption yield (Y) and adsorption capacity (q_e) both decreased as the initial concentration of methylene blue increased. At lower concentrations, activated biochar effectively removed a higher percentage of methylene blue due to the availability of sufficient active sites relative to the adsorbate molecules. However, at higher concentrations, the active sites became saturated, reducing the removal efficiency and adsorption capacity. At an initial concentration of 3 mg/L, the greatest yield and adsorption capacity were obtained, with R=99.12% and q_e=19.83 mg/g, respectively. On the other hand, the yield and adsorption capacity dropped to 96% and 19.2 mg/g, respectively, at higher concentrations (9 mg/L). This pattern emphasized how crucial it was to enhance the methylene blue starting concentration in order to optimize activated biochar's adsorption capabilities. The observed pattern was consistent with earlier research suggesting that adsorption efficiency was mostly determined by the ratio of accessible adsorption sites to adsorbate molecules. These results indicated that while activated biochar performed well at low concentrations, site saturation caused it to lose some of its adsorption capacity at higher concentrations. Therefore, in practical situations, adjusting adsorbent dosage and regulating initial concentration were necessary to maximize removal efficiency.

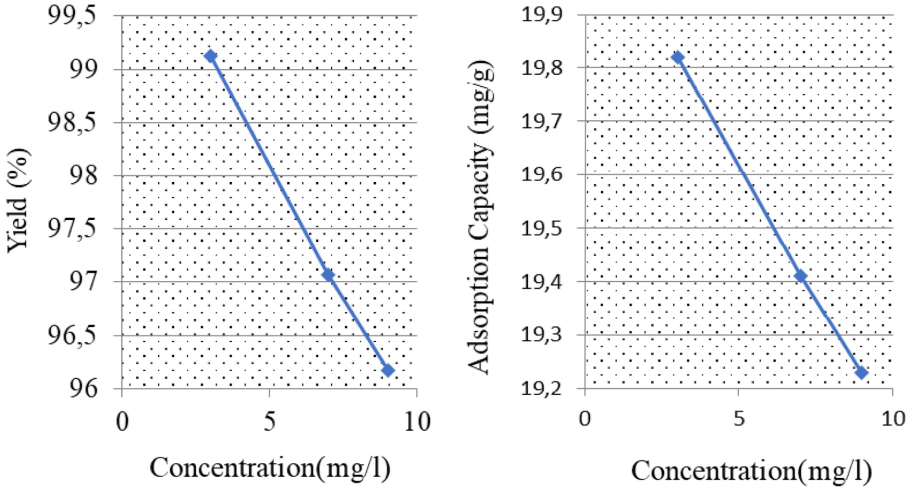

Fig. 8. Yield and adsorption capacity of methylene blue on activated biochar (ABC) as a function of concentration.

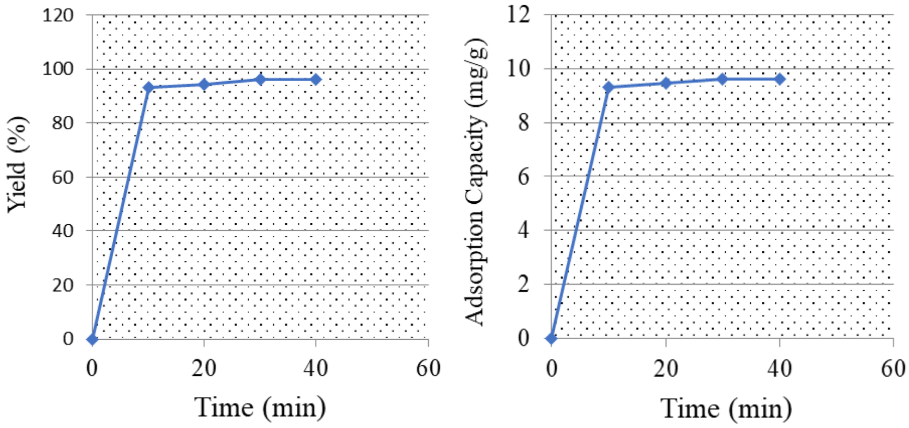

Fig. 9. Effect of stirring time on yield and adsorption capacity of methylene blue onto activated biochar (ABC).

3-2-4. Contact time effect on the adsorption efficiency

Figure 9 illustrates the relationship between stirring time and both adsorption yield (Y) and adsorption capacity (q_e). The data showed that both Y and q_e increased rapidly during the initial 10 minutes of stirring, after which the curves plateau, indicating that equilibrium has been reached. Beyond 10 minutes, no significant changes in adsorption performance were observed, with Y and q_e remaining nearly constant up to 60 minutes. At equilibrium, the adsorption yield reached 96.16%, and the adsorption capacity stabilized at 9.61 mg/g. The rapid adsorption within the first 10 minutes could be attributed to the higher availability of active sites on the biochar surface, which facilitated the rapid uptake of MB molecules. This phenomenon can also be explained by the biochar surface's active sites becoming saturated, which reduced the number of sites available for further adsorption. One typical feature of adsorption research was the change from a fast to a slower adsorption phase, which signified the creation of an equilibrium state, which was in agreement with Malbenia John et al. (2024) [37]. These findings implied that methylene blue adsorption onto activated biochar was extremely effective and time-efficient, reaching peak performance in a brief amount of stirring time. The results emphasized how crucial it was to maximize contact duration in order to reduce energy consumption and operating expenses without sacrificing adsorption effectiveness.

3-2-5. Adsorption temperature effect

The effect of adsorption temperature on the performance of activated biochar (ABC) was evaluated by using three beakers, each containing 250 mL of methylene blue (MB) solution with an initial concentration of 3.0 mg/L. The adsorption temperature was set at 10 °C, 20 °C, and 40 °C for each beaker, and the results are illustrated in Fig. 10a and Fig. 10b.

a. Without Filtration

After stirring the samples for 50 minutes at 200 rpm, the solutions were allowed to settle for 30 minutes. The adsorption yield (Y) and adsorption capacity (q_e) were measured directly from the decanted solution. Fig. 10a shows that as the adsorption temperature increased, the adsorption capacity also increased, reaching a maximum value of 9.8 mg/g at 40 °C. The increase in adsorption capacity with temperature

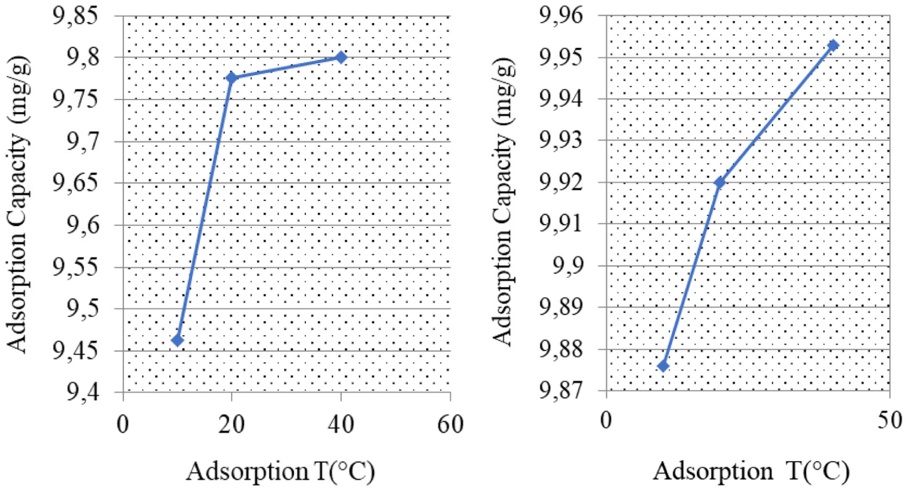

Fig. 10. Adsorption temperature effect of on Yield and Methylene Blue Adsorption Capacity Using Activated Biochar (ABC): (a) Without Filtration, (b) With Filtration.

Table 3. Adsorption capacity of methylene blue (MB) by various adsorbents

Adsorbent Types	Maximum adsorption (mg/g)	Reference
Activated biochar (ABC) of date seeds	19.83	This study
Black Carbon of shells of apricot kernels	13.88	[38]
Activated carbon from grape wood wastes	5.88	[17]

suggested that higher temperatures enhanced the diffusion of MB molecules into the biochar pores, thereby improving adsorption efficiency.

b. With Filtration

In a parallel process, the decanted samples were filtered using 0.45 μm filter paper to recover the activated biochar. The adsorption yield and capacity were measured after filtration, with the results presented in Fig. 11b. Similar to the results without filtration, the adsorption capacity increased with temperature, achieving a maximum value of 9.96 mg/g at 40 °C. The filtration process ensured the complete recovery of biochar and eliminated suspended particles, leading to slightly higher adsorption capacity measurements compared to the unfiltered samples.

These results suggested that temperature significantly affected activated biochar's adsorption capacity. The stronger molecular interaction and higher kinetic energy of MB molecules, which promoted their diffusion into the biochar pores, were responsible for the higher adsorption capacity at higher temperatures. Higher temperatures were advantageous for increasing the removal effectiveness of methylene blue, as this characteristic implied that the adsorption process was endothermic in nature.

3-3. Comparison of ABC With Other Adsorbents

Activated biochar (ABC) fabricated from date seeds demonstrated superior adsorption performance compared to other adsorbents reported in the literature, as shown in Table 3. The adsorption capacity of ABC for methylene blue (MB) reached a maximum value of 19.83 mg/g, significantly exceeding the capacities of other bio-based adsorbents. For example, black carbon derived from apricot kernel shells exhibited a maximum adsorption capacity of 13.88 mg/g [37], while activated carbon prepared from grape wood wastes showed a much lower capacity of 5.88 mg/g [38].

The enhanced performance of ABC can be attributed to its optimized activation process, particularly the use of $ZnCl_2$ as an activator and high-temperature pyrolysis at 1000 °C. These factors promoted the formation of a highly porous structure with a large surface area and abundant active sites, which were essential for efficient adsorption. In contrast, the lower adsorption capacities of other adsorbents may result from less efficient activation methods, lower surface area, and insufficient pore development. This comparison proved the efficacy of ABC produced from date seeds as a highly effective and sustainable adsorbent for the removal of methylene blue. Its exceptional performance showed the benefit of using agricultural left overs to create high-performance adsorbents and underscored its potential for environmental applications, especially in wastewater treatment.

4. Conclusion

This study showed that date-seed-derived activated charcoal (ABC) has a maximum adsorption capacity of 19.83 mg/g and a yield of 99.15%, making it an extremely effective adsorbent for the removal of methylene blue (MB). Activation temperature, particle size, activator type, and initial MB concentration were among the factors that affected the adsorption performance. At 1000 °C, the maximum adsorption efficiency was recorded, and equilibrium was reached after 60 minutes. These findings supported the promise of ABC made from date seeds as an economical and effective wastewater treatment method. The results effectively illustrated the role that temperature, activator type, and other variables played in adsorption performance, offering important new information for improving materials based on biochar. The findings emphasized the significance of the structural characteristics of biochar, including its porosity and surface area, which were greatly improved by chemical activation and high-temperature treatment. Due to these qualities, ABC was a material that showed promise for environmental restoration and was consistent with sustainability objectives. Future studies should concentrate on the stability and reusability of ABC, particularly examining its capacity for regeneration and long-term performance across several adsorption cycles. By tackling environmental issues, this strategy not only makes ABC more practicable but also supported worldwide sustainability objectives. These initiatives foster creative and sustainable approaches to wastewater treatment and the conversion of agricultural waste into high-value resources by supporting SDG 6 and SDG 12 (Responsible Consumption and Production).

Acknowledgement

The authors would like to express their gratitude to the Algerian Ministry of Higher Education and Scientific Research for their financial and institutional support of this work. Special thanks are also extended to our collaborators from Universiti Kebangsaan Malaysia (UKM) for their valuable contributions and assistance throughout this study.

References

1. Korak, J. A., Huggins, R. and Arias-Paic, M., "Regeneration of Pilot-Scale Ion Exchange Columns for Hexavalent Chromium Removal," *Water Res*., **118**, 141-15(2017).
2. Mohan, D. and Pittman, C. U., "Activated Carbons and Low-Cost Adsorbents for Remediation of Tri- and Hexavalent Chromium from Water," *J. Hazard. Mater*., **137**, 762-811(2006).

3. Lemoine, A. and Tounian, P., "Allergie Aux Colorants Alimentaires: Une Pathologie À Évoquer Avec Parcimonie," *Rev. Fr. Allergol. Elsevier*, **58**(7), 506-512(2018).
4. Gohar, J., Naeem, A., Farah, D., Tahir, B., Shafaq, J. and Sadaf, S., "Efficient Removal of Dyes in Textile Effluents Using Aluminum-Based Coagulant," *Rev. Fr. Allergol. Elsevier*, **7**(3), 197-207(2021).
5. Brower, G. R. and Reed, G. D., "Economical Pre-treatment for Color Removal from Textile Dye Wastes," In: Proc. 41st Industrial Waste Conference, Purdue University: West Lafayette, Indiana, 612(1985).
6. Majewska-Nowak, K., "Effect of Flow Conditions on Ultrafiltration Efficiency of Dye Solutions and Textile Effluents," *Desalination*, **71**(2), 127-135(1989).
7. Shendrik, O. R., "Electro Membrane Removal of Organic Dyes from Wastewaters," *Kimiyi Technology Vody*, **11**, 467-472(1989).
8. Ding, Z., Min, C. W. and Hui, W. Q., "A Study on the Use of Bipolar Particles – electrode in the Decolorization of Dyeing Effluents and Its Principle," *Water Sci. Technol.*, **19**(3/4), 39-42(1987).
9. Jawad, A. H., Al-Heetimi, D. T. A. and Mastuli, M. S., "Biochar from Orange (Citrus Sinensis) Peels by Acid Activation for Methylene Blue Adsorption," *Iran. J. Chem. Chem. Eng.*, **38**, 291-105(2019).
10. Nawawi, W. I. W., Ain, S. K., Zaharudin, R., Jawad, A. H., Ishak, M. A. N., Ismail, S. K. and Sahid, S., "New TiO_2/DSAT Immobilization System for Photodegradation of Anionic and Cationic Dyes," *Int. J. Photoenergy*, **3**, 1-6(2015).
11. Coia-Ahlman, S. and Groff, K. A., "Textile Wastes," *J. Water Polut. Control Fed.*, **62**, 473-478(1990).
12. Zbair, M., Ahsaine, H. A. and Anfar, Z. J., "Porous Carbon by Microwave-Assisted Pyrolysis: An Effective and Low-Cost Adsorbent for Sulfamethoxazole Adsorption and Optimization Using Response Surface Methodology," *Journal of Cleaner Prod.*, **202**, 571-581(2018).
13. Basha, N. A., Rathinavel, T. and Sridharan, H., "Activated Carbon from Coconut Shell: Synthesis and Its Commercial Applications - A Recent Review," *Appl. Sci. Eng. Prog.*, **16**(2), 2022(2023).
14. Chebbi, R., Fadel, A. and Aidi, A., "The Elimination by Natural Algerian Clay of Chromium Ions from Salt Water," *Ann. Chim. - Sci. Mat.*, **45**(2), 105-112(2021).
15. Yamin, Y., Hussein, M. Z. and Ahmad, F., "Adsorption of Methylene Blue onto Treated Activated Carbon," *Malays. J. Anal. Sci.*, **11**(11), 400-406(2007).
16. Seyed, A. M., Davood, S., Arezoo, Mand. and Parastoo, D., "Methylene Blue Removal Using Prepared Activated Carbon from Grape Wood Wastes: Adsorption Process Analysis and Modeling," *Water Qua. Res. J.*, **57**(1), 1-19(2021).
17. Tran, H. N., Wen, Y. C., Wang, Y. F. and You, S. J., "Highly Efficient Removal of Hazardous Aromatic Pollutants by Micro-Nano Spherical Carbons Synthesized from Different Chemical Activation Methods: A Comparison Study," *Environ. Technol.*, **40**, 1376-1391(2019).
18. Ammar Fadel, Saci Nacef, "Examination of an Algerian Clay in the Retention of Zinc Ions Chargedin Brackish Water," *Korean Chem. Eng. Res.*, **55**(5), 685-689(2017).
19. Bounoukta, C. E., Megías-Sayago, C., Navarro, J. C., Ammari, F., Ivanova, S., Centeno, M. Á. and Odriozola, J. A., "Functionalized Biochars as Supports for Ru/C Catalysts: Tunable and Efficient Materials for γ-Valerolactone Production," *Nanomaterials*, **13**(6), 1129(2023).
20. MacHado, L. M. M., Lütke, S. F., Perondi, D., Godinho, M., Oliveira, M. L. S., Collazzo, G. C. and Dotto, G. L., "Treatment of Effluents Containing 2-Chlorophenol by Adsorption Onto Chemically and Physically Activated Biochars," *J. Environ. Chem. Eng.*, **8**(6), 104473(2020).
21. Sujiono, E. H., Zabrian, D., Zurnansyah, Mulyati, V., Zharvan, and Samnur, N. A., "Fabrication and Characterization of Coconut Shell Activated Carbon Using Variation Chemical Activation for Wastewater Treatment Applications," *Results Chem.*, **4**, 100291 (2022).
22. Byamba-Ochir, N., Buyankhishig, B., Byambasuren, N. and Surenjav, E., "Characterization of Silver Loaded Activated Carbon Prepared Under Supercritical Water Conditions," *Solid State Phenomena*, **288**, 59-64(2019).
23. Freitas, J. V., Nogueira, F. G. E. and Farinas, C. S., "Coconut Shell Activated Carbon as an Alternative Adsorbent Inhibitor from Lignocellulosic Biomass Pretreatment," *Ind. Crop. Prod.*, **137**(12), 16-23(2019).
24. Asep Bayu Dani Nandiyanto, Rosi Oktiani, Risti Ragadh., "How to Read and Interpret FTIR Spectroscope of Organic Material," *Journal of Science Technology*, **4**(1), 97-118(2019).
25. Pallarés, J., González-Cencerrado, A. and Arauzo, I., "Production and Characterization of Activated Carbon from Barley Straw by Physical Activation with Carbon Dioxide and Steam," *Biomass Bioenergy*, **115**, 64-73(2018).
26. Xinkai, L., Wang, Y., Zhang, G., Sun, W., Bai, Y., Zheng, L., Han, X. and Wu, L. E., "Influence of Mg-Promoted Ni-Based Catalyst Supported on Coconut Shell Carbon for CO_2 Methanation," *Chemistry Select*, **4**(3), 838-845(2019).
27. Hong, Z., Zhong, F., Niu, W., Zhang, K., Su, J., Liu, J., Li, L. and Wu, F., "Effects of Temperature and Particle Size on the Compositions, Energy Conversions, and Structural Characteristics of Pyrolysis Products from Different Crop Residues," *Energy*, **190**, 116413(2020).
28. Lin, F., Liu, X., Ma, M., Qi, F., Pan, Y., Wang, L., Ma, P. and Zhang, Y., "Real-Time Monitoring the Carbonization and Activation Process of Activated Carbon Prepared from Chinese Parasol via Zinc Chloride Activation," *J. Anal. Appl. Pyrol.*, **155**, 105089(2021).
29. Park, J. H., Ok, Y. S., Kim, S. H., Cho, J. S., Heo, J. S., Delaune, R. D. and Seo, D. C., "Evaluation of Phosphorus Adsorption Capacity of Sesame Straw Biochar on Aqueous Solution: Influence of Activation Methods and Pyrolysis Temperatures," *Environ. Geochem. Health*, **37**(6), 969-983(2015).
30. Towfik, A. Saleh, "Simultaneous Adsorptive Desulfurization of Diesel Fuel over Bimetallic Nanoparticles Loaded on Activated Carbon," *J. Clean. Prod.*, **172**, 2123-2132(2018).
31. Wang, X., Li, C., Li, Z., Yu, G. and Wang, Y., "Effect of Pyrolysis Temperature on Characteristics, Chemical Speciation, and Risk Evaluation of Heavy Metals in Biochar Derived from Textile Dyeing Sludge," *Ecotoxicol. Environ. Saf.*, **168**, 45-52(2019).
32. Dehkhoda, A. M., Ellis, N. and Gyenge, E., "Effect of Activated Biochar Porous Structure on the Capacitive Deionization of NaCl and $ZnCl_2$ Solutions," *Microporous Mesoporous Mater.*, **224**, 217-228(2016).

33. Wang, H., Xie, R., Zhang, J. and Zhao, J., "Preparation and Characterization of Distillers' Grain-Based Activated Carbon as a Low-Cost Methylene Blue Adsorbent: Mass Transfer and Equilibrium Modeling," *Adv. Powder. Technol*., **29**(1), 27-35(2018).
34. Wang, J., Wang, R., Ma, J. and Sun, Y., "Study on the Application of Shell-Activated Carbon for the Adsorption of Dyes and Antibiotics," *Water*, **14**(22), 3752(2022).
35. Suárez-García, F., Martínez-Alonso, A. and Tascón, J. M. D., "A Comparative Study of the Thermal Decomposition of Apple Pulp in the Absence and Presence of Phosphoric Acid," *Polym Degrad Stab*., **75**, 375-383(2002).
36. Malbenia, J. M., Benettayeb, A., Belkacem, M., Ruvimbo Mitchel, C., Hadj Brahim, M., Benettayeb, I., Haddou, B., Al-Farraj, S., Alkahtane, A. A., Ghosh, S., Chia, C. H., Sillanpaa, M., Baigenzhenov, O. and Hosseini-Bandegharaei, A., "An Overview on the Key Advantages and Limitations of Batch and Dynamic Modes of Biosorption of Metal Ions," *Chemosphere*, **357**(4), 142051(2024).
37. Fadel, A., Chebbi, R., Aidi, A. and Azri, N., "Kinetics and Isotherms Modeling of Methylene Blue Adsorption by Black Carbon Using the Shells of Apricot Kernels," *Indian J. Chem. Technolo*., **28**(4), 412-420(2021).

Authors

Chebbi Rachid: Chemical and Environmental Process Engineering Laboratory, University of Biskra, PO Box 145, Biskra, 07000, Algeria; r.chebbi@univ-biskra.dz

Fadel Ammar: Chemical and Environmental Process Engineering Laboratory, University of Biskra, PO Box 145, Biskra, 07000, Algeria; am.fadel@univ-biskra.dz

Souifi Imane: Chemical and Environmental Process Engineering Laboratory, University of Biskra, PO Box 145, Biskra, 07000, Algeria; imanesouifi20@gmail.com

Salma Samidin: Department of Chemical and Process Engineering, Faculty of Engineering and Built Environment,Universiti Kebangsaan Malaysia, 43600 UKM Bangi, Selangor, Malaysia; salma_samidin@yahoo.com

Wan Nor Roslam Wan Isahak: Department of Chemical and Process Engineering, Faculty of Engineering and Built Environment, Universiti Kebangsaan Malaysia, 43600 UKM Bangi, Selangor, Malaysia; wannorroslam@ukm.edu.my